



Received: 28 May, 2024

Accepted: 11 June, 2024

Published: 12 June, 2024

\*Corresponding author: Mariia I Terebinska, Institute of Micro/Nano Materials and Devices, Ningbo University of Technology, China,  
E-mail: [li\\_sanming@sina.com](mailto:li_sanming@sina.com); [terebinska@ukr.net](mailto:terebinska@ukr.net)

ORCID: <https://orcid.org/0000-0002-5635-7653>

**Keywords:** Hydrophilic and hydrophobic silica; c succinic acid; Composite system; <sup>1</sup>H NMR spectroscopy; Interfacial energy

**Copyright License:** © 2024 Krupska TV, et al. This is an open-access article distributed under the terms of the Creative Commons Attribution License, which permits unrestricted use, distribution, and reproduction in any medium, provided the original author and source are credited.

<https://www.chemisgroup.us>

Check for updates

## Research Article

# Construction of composites for medical purpose based on pyrogenic silica with immobilized succinic acid and their properties

Tetyana V Krupska<sup>1,2</sup>, Mariia I Terebinska<sup>1\*</sup>, Nataliia Yu Klymenko<sup>1,2</sup>, Nadiia V Vitiuk<sup>1,2</sup>, Qiliang Wei<sup>1</sup>, Jinju Zheng<sup>1</sup>, Weiyou Yang<sup>1</sup> and Volodymyr V Turov<sup>1,2</sup>

<sup>1</sup>Institute of Micro/Nano Materials and Devices, Ningbo University of Technology, Ningbo City, 315211, P.R. China

<sup>2</sup>Chuiko Institute of Surface Chemistry of National Academy of Sciences of Ukraine, 17 General Naumov Str., Kyiv, 03164, Ukraine

## Abstract

The work is aimed at creating new, more effective drugs containing succinic acid. For this purpose, a methodology has been developed for transferring the active substance to a nano-sized state, in which the acid, due to an increase in its outer surface, is in the form of clusters, which, upon contact with the mucous membrane, can be more easily absorbed by the body. A complex of physicochemical methods was used to study the effect of immobilization of Succinic Acid (SA) on the surface of hydrophilic, hydrophobic silica and their mixtures on the existing specific surface area and the state of the adsorption layer. It has been shown that during the joint mechanical grinding of crystalline succinic acid with silicas, composite systems are formed in which it is uniformly distributed in the interparticle gaps of silicas and is in the form of nanosized predominantly amorphous clusters. For silicas and their mixtures, the signal of acid crystallites is also fixed on the X-ray diffraction patterns. Additional mechanical treatment of composites with water practically does not change the ratio of amorphous and crystalline components of succinic acid in the surface layer, which indicates its poor solubility in clustered water. This is also confirmed by liquid NMR data, according to which there is no signal from the methylene groups of succinic acid in the spectra. All composites, regardless of the content of SA, treatment with water, and the ratio of the hydrophobic and hydrophilic components, retain a high adsorption capacity with respect to nitrogen. The BET-specific surface of the composites remains at the level of 150 - 200 m<sup>2</sup>/g. Hydrated forms of hydrophobic silica AM-1 retain the ability to interact with non-polar substances. Using chloroform as an example, it was shown that even at h = 1 g/g, chloroform displaces part of the water from the interparticle space, which manifests itself in a decrease in the interfacial energy of water due to the formation of surface water clusters with a large radius. The hydrophobic silica surface stabilizes the weakly associated form of water, the amount of which can reach 20 mg/g.

## Introduction

Nanopharmacology includes the use of nanoparticles, quantum dots, carbon nanotubes, and gold and silver nanoparticles for pharmacological purposes, and their joint use with traditional pharmaceutical remedies, as well as the study of the effect of nanoparticles on metabolic processes. Nanopharmacology is especially actively developing in the field of creating new types of anticancer drugs, means of drug delivery to the target, and building complex multilevel

drugs, for example, using liposomes, monoclonal antibodies, magnetic carriers, etc. [1-6].

The creation of new types of polyfunctional materials that can be used in biotechnological schemes and the latest materials for biomedical purposes can be achieved through the development of composite systems that include hydrophilic and (or) hydrophobic highly dispersed materials, organic substances of various chemical nature, water and some types of compounds (activators), giving them predefined properties.

In complex heterogeneous systems, their adsorption and technological characteristics largely depend on self-consistent processes that occur during the formation of a composite, that is, the formation of supramolecular systems with a minimum value of thermodynamic potentials. These effects can be used to develop ways to control the properties of a composite system by varying its hydrophobic-hydrophilic interactions, the processes of cluster formation of aqueous and aqueous-organic systems that make up composites, and influencing the phase state of the components [7,8]. Sufficiently technological methods have been developed for transferring hydrophobic highly dispersed adsorbents to a strongly hydrated state [9,10], which can serve as a technological basis for the preparation of complex heterogeneous systems for their use in aqueous media, which are the basis of most biological fluids.

Unlike liquids, solid particles with different hydrophobic-hydrophilic properties (in a dry state) after mechanical mixing can form an almost homogeneous mixture in which both types of particles are part of common aggregates and interact in them through Van der Waals forces. In this case, the difference in the interaction energies of hydrophobic, hydrophilic, and mixed particles is small. However, the possibility of joint coexistence of dissimilar particles in the volume can be violated when a liquid phase (surfactant, water, or hydrophobic liquid) is added [11-14]. Spontaneous separation of components in mixtures of powders or viscous liquids (microcoagulation) caused by Brownian motion cannot occur or is very slow, however, this process can be significantly accelerated under the influence of a mechanical load applied to the composite system during its mixing, especially in the presence of surfactant. Since coagulation reduces the free energy of a multicomponent system, it should lead to an increase in the binding energy of liquid components to the surface of dispersed particles. This effect can be used for structural modification of the mineral component of the composite system.

In the works of last year [15-17], it has been shown that water adsorption in oxide nanostructured materials occurs according to the mechanism of cluster formation, in which no individual molecules are adsorbed on the primary centers of the surface, but clusters, the size of which is determined by the morphology of interparticle gaps and the hydrophobic-hydrophilic properties of the surface. Clustered water has a number of unusual properties that distinguish it from bulk water: for example, polar organic substances, including mineral acids, are poorly soluble in nanosized water clusters. A weakly polar medium, even in hydrophilic materials, can displace water, replacing it near the surface, which leads to an increase in the average radius of adsorbed water clusters. Since for any substances, the decrease in linear sizes is accompanied by an increase in surface energy, it can be expected that when adsorbed substances are transferred to a nanoscale clustered state, such processes as dissolution (solubilization) will occur with lower energy costs. Therefore, on the basis of mixtures of hydrophobic and hydrophilic silicas taken in a certain proportion, polyfunctional composite systems for medical purposes can be created. The process of activation of biologically active substances by transferring them to a

clustered state will take place in them, transportation to the place of their absorption by the body, and creation of an area of increased bioavailability in the absorption zone due to local changes in the structure of water. First, the desorption of the delivered substances occurs. After that, the mineral matrix will be able to adsorb metabolic products and toxins, which will later be removed from the body naturally.

The aim of this work was to study the effect of mechanochemical immobilization of a biologically active component, its amount, the presence of water and the ratio of the hydrophobic and hydrophilic components of the mineral matrix on the adsorption properties of the material, the crystallinity of the adsorption layer, the structure of the interfacial water, its parameters of interaction with the matrix (on the example of designing composites of hydrophobic and hydrophilic silicas with succinic acid ( $\text{COOHCH}_2\text{CH}_2\text{COOH}$ )). The work is aimed at creating new, more effective drugs containing succinic acid. For this purpose, a methodology has been developed for transferring the active substance to a nano-sized state, in which the acid, due to an increase in its outer surface, is in the form of clusters, which, upon contact with the mucous membrane, can be more easily absorbed by the body.

Succinic Acid (SA) is one of the simplest dicarboxylic acids. It was first isolated from natural amber, although it is currently synthesized mainly by biotechnological methods [18-21] and has many useful properties, which leads to its use in a number of medical and cosmetic drugs. Succinic acid is readily soluble in water and some polar organic solvents, but practically insoluble in chloroform, hexane, and other non-polar or slightly polar liquids. Currently, there are several types of drugs on the market based on succinic acid and hydrophilic adsorbents, such as silicas or clay minerals, used to treat alcoholism, osteoporosis, and other diseases [22,23].

Succinic acid takes part in energy production: it supports the functioning of mitochondria, cellular respiration processes, and the synthesis of ATP – the most important source of energy. It has been used as a medicine for many centuries. Initially, dry crushed amber was used, some types of which can contain up to 10% succinic acid. Currently, chemical and microbiological methods for the production of succinic acid are used, which makes its use cheaper. Although succinic acid is synthesized in the human body during metabolism, in many cases its natural concentration may not be sufficient. A promising way of introducing it into the body may be immobilization on the surface of highly dispersed silica, which, along with its transport function, can act as an adsorbent (cleansing the body of excess toxins), a source of silicon (participating in the formation of nerve fibers) and a structuring agent, which, when in contact with hydrophobic areas the surface of the mucous membrane transfers the water associated with it into a weakly associated state, which promotes more active dissolution of both polar and non-polar substances, thereby accelerating cellular metabolism.

Succinic acid, like other organic acids, is an active chemical compound and in some cases, at high concentrations, can have a negative effect on the walls of the stomach and intestines.

To reduce the potentially harmful effects of concentrated acid, it can be converted into a weakly bound state with a silica carrier. Moreover, after entering the body, areas with a superconcentrated solution of succinic acid will not be created on the internal walls of the digestive tract. Therefore, it can be expected that the use of silica-succinic acid composites will help eliminate negative side effects.

## Materials

Pyrogenic silica A-300 and methylsilica AM-1 (Kalush, Ukraine) were used as mineral carriers. Methylsilica AM-1 was synthesized by replacing the surface hydroxyl groups of hydrophilic silica A-200 with dimethylsilyl groups [24]. The resulting product is hydrophobic and even at 100% humidity it is able to adsorb only small (up to 5%) amounts of water from the air. Dry powder of the original silica A-300 (300 m<sup>2</sup>/g) was used to obtain the wetting-drying process (1 g of silica was wetted with 3 g of water). This sample was kept in a sealed container for three days at room temperature and then dried at 120 °C for six hours. Crystalline succinic acid (10 or 20 wt.%) was added to wetting-drying silica A-300, AM-1 and mixture A-300/AM-1 (1:1) and mixed under mechanical action for 20–30 minutes until homogeneous systems were obtained. Then distilled water was added to the samples (0.9 g of water per 1 g of solid substance) and A-300/SA/water was mixed for 5 min, A-300/AM-1/SA/water for 10 – 15 min, AM-1/SA/water 20–25 min. It should be noted that all systems remained in a powdery state because the amount of water added was small and no gelation occurred. In this case, SA is uniformly distributed over the surface of methylsilica particles, becomes largely amorphous, and creates water adsorption centers on the surface of the hydrophobic material. Composites AM-1/SA, (AM-1+A-300)/SA, like the initial methylsilica, continue to retain hydrophobic properties. They do not mix with water. Adding water to them in equal-weight amounts creates a heterogeneous system in which it is in the form of a separate phase in a powdery hydrophobic medium. However, if such a composite is subjected to high mechanical loads, for example, by grinding in a porcelain mortar, then the system becomes homogeneous, and its density increases to 1000 mg/cm<sup>3</sup>. After removing the composite from the walls of the mortar, it takes the form of a wet powder, which indicates the removal of air from the interparticle gaps and its replacement with water.

We studied 15 samples (Table 1) prepared under the same conditions. The amount of SA immobilized on the surface was 100 or 200 mg/g dry adsorbent. The aim of the research was to determine to what extent immobilization carried out in dry and humid conditions affects the adsorption characteristics of adsorbents and the crystallinity of the organic phase, whether it depends on the hydrophobic properties of the mineral component of the composite. The crystallinity of succinic acid was determined by X-ray phase analysis and TEM electron microscopy. Structural characteristics of adsorbents were determined on the basis of nitrogen adsorption-desorption isotherms taken at 77.4 K.

To analyze the textural characteristics of individual and mixed samples degassed at 110 °C for 12 h, low temperature

(77.4 K) nitrogen adsorption-desorption isotherms were recorded using a Micromeritics ASAP 2460 adsorption analyzer. The specific surface area was calculated according to the standard BET method at  $0.05 < p/p_0 < 0.3$  (using Micromeritics software).

Powder X-Ray Diffraction (XRD) patterns were recorded using a D8 Advance X-ray. Diffractometer (Bruker AXS) in Bragg-Brentano geometry (Cu K $\alpha$  1 radiation,  $\lambda = 0.15406$  nm). Diffraction data were typically collected at  $2\theta$  in the 5 – 90° range at a step of 2°/min.

Transmission electron microscopy, TEM (TECNAI G2 F30 microscope (FEI-Philips, operating voltage 300 kV) was used to analyze the particulate morphology of samples. The powder samples were added to acetone (chromatographic grade) and sonicated. A suspension drop was then deposited onto a copper grid covered by a thin carbon film. After acetone evaporation, the dry sample remaining on the film was studied.

Solid-state <sup>1</sup>H Magic-Angle Spinning (MAS) NMR spectra were recorded using an Agilent DD2 600 MHz NMR spectrometer (Agilent, USA, magnetic field strength 14.157 T). A powder sample was placed in a pencil-type zirconia rotor of 4.0 mm o.d. The spectra were recorded at a spinning speed of 8 kHz with a recycle delay of 5 s. The adamantane was used as the reference of the <sup>1</sup>H chemical shift of proton resonance ( $\delta_H$ ).

Solid-state <sup>29</sup>Si cross-polarization (CP)/MAS NMR spectra were recorded using the same NMR spectrometer at a resonance frequency of 199.13 MHz for <sup>29</sup>Si using CP/MAS and high-power <sup>1</sup>H decoupling. The spectra were recorded at a spinning speed of 8 kHz (4  $\mu$ s 90° pulses), 2 ms CP pulse, and a recycle delay of 3 s. The Si signal of tetramethylsilane (TMS) at 0 ppm was used as the reference for the <sup>29</sup>Si chemical shift ( $\delta(^{29}\text{Si})$ ).

## Results and discussion

The adsorption isotherm of the A-300 sample with 200 mg/g of succinic acid immobilized on its surface is shown as an example in Figure 1. The shape of the isotherm is typical for mesoporous adsorbents [25,26]. Despite the fact that pyrogenic silicas are non-porous materials, due to strong interparticle interactions, primary particles form aggregates

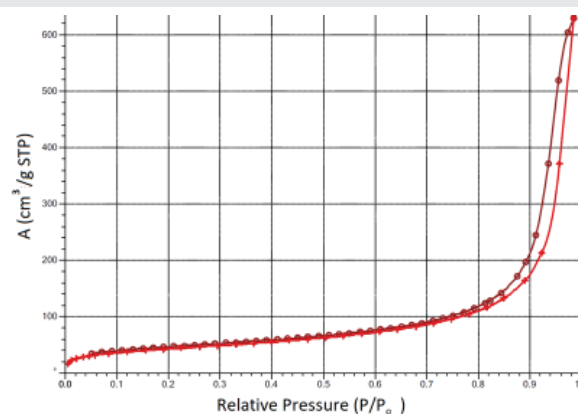


Figure 1: Recorded at 77.4 K nitrogen adsorption-desorption isotherm for sample A-300/20 wt. % succinic acid (Micromeritics ASAP 2460 adsorption analyzer).

and agglomerates, in which interparticle gaps form secondary pores. The porous structure of such nanomaterials is not rigid and can change during technological processing, in particular, during immobilization on the surface of various substances, the wetting-drying process, or compaction by mechanical loads [27–29].

It was shown that SA immobilization reduces the specific surface area and total pore volume of composite systems (Table 1). This indicates the rearrangement of silica aggregates during mechanochemical treatment with crystalline SA. An increase in the amount of acid in the composite from 100 to 200 mg/g is accompanied by a slight decrease in the measured specific surface area. It could be expected that the mechanical treatment of silica composites with water, the amount of which is almost an order of magnitude greater than the amount of acid, would lead to a significant rearrangement of the composite systems and a decrease in their specific surface after thermal vacuum drying, which precedes the measurement of the specific surface. However, this does not happen. Moreover, for some samples, after contact with water, there is a tendency to increase the specific surface area. Consequently, SA immobilization does not lead to too large a decrease in the specific surface area of composite systems, which makes it possible to count on a sufficiently high adsorption activity of materials when they enter the biological environment.

The results of studying some samples by X-ray phase analysis and transmission electron microscopy are shown in Figure 2. Carefully ground succinic acid, even at high magnification (Figure 2a), is observed as a crystalline substance in which the crystal size exceeds 100 nm. In the case of immobilization on the surface of silicas or their mixtures, the crystallinity of SA cardinally decreases. Although residual peaks of the crystalline phase are observed on the X-ray patterns, the main part of the acid passes into the amorphous state, which is also evidenced by the absence of its visible crystals in the TEM photographs

**Table 1:** Effect of succinic acid adsorption on the characteristics of the porous structure of silicas A-300, AM-1, and their mixtures (Micromeritics ASAP 2460 adsorption analyzer).

Sample	$C_{SA}$ (wt. %)	$S_{BET}$ (m <sup>2</sup> /g)	$V_p$ (cm <sup>3</sup> /g)	$R$ (nm)
A-300	10	172	1.10	25.0
	20	153	0.49	12.7
AM-1	10	128	0.79	24.0
	20	127	0.28	8.8
A-300/AM-1 1/1	10	164	0.88	21.0
	20	130	0.35	11.0
A-300/H <sub>2</sub> O	10	219	0.71	12.8
	20	159	0.59	15.0
AM-1/H <sub>2</sub> O	10	136	0.67	19.8
	20	123	0.43	13.8
A-300/AM-1 1/1/H <sub>2</sub> O	10	160	0.84	20.9
	20	141	0.51	14.4
A-300/AM-1 1/1	-	200	0.89	17.8
A-300/AM-1 1/1/H <sub>2</sub> O	-	216	0.75	13.8
AM-1	-	172	0.73	17.0

**Note:**  $C_{SA}$  (wt. %) - concentration of succinic acid in the sample;  $S_{BET}$ , m<sup>2</sup>/g - the surface area estimated by the BET method;  $V_p$  (cm<sup>3</sup>/g) - total pore volume estimated by the BET method;  $R$  (nm) - pore radius A-300 - hydrophilic silica; AM-1 - hydrophobic silica; A-300/AM-1 is a mixture of hydrophilic and hydrophobic silicas in a 1:1 ratio.

(Figure 2b–e). The signal intensity of the crystalline form of SA increases with an increase in its amount in the composite (Figure 2c,e). It should be noted that this increase in intensity may not be associated with a decrease in the degree of amorphization, but only with an increase in the amount of SA.

The X-ray pattern and TEM micrograph of AM-1 methylsilica are shown in Figure 2e. Only the amorphous silica signal is present on it. It could be expected that the presence of a large amount of water in the samples would change the form of X-ray diffraction patterns due to the dissolution of SA in the interfacial water (Figure 3). It turned out that this did not happen. For this and other samples recorded in the presence of water, the intensity of the crystalline SA signals is practically independent of the presence of water. Consequently, crystalline SA practically does not dissolve in clustered water and they exist as two independent phases.

<sup>29</sup>Si solid-state MAS NMR spectra of A-300 and AM-1 silicas and their mixtures with SA immobilized on the surface, as well as the initial AM-1, are shown in Figure 4. The spectrum of A-300 shows three signals with chemical shifts in the range  $\delta_{Si} = -120 -100$  ppm, which refer to silicon atoms bonded to four, three, and two oxygen atoms (Q<sub>4</sub>, Q<sub>3</sub>, and Q<sub>2</sub>, respectively). For samples containing AM-1, in addition to these signals, a silicon signal is observed from dimethylsilyl groups with a chemical shift  $\delta_{Si} = -15$  ppm.

The <sup>1</sup>H NMR spectra show that proton signals of adsorbed (immobilized) substances are recorded simultaneously with the solid phase (Figure 5). For sample A-300 + 100 mg/g SA (Figure 5a), which contained up to 80 mg/g residual water, the spectra show signals of the methylene groups of the acid ( $\delta_H = 3$  ppm), the total signal of water, and COOH of acid protons ( $\delta_H = 6$  ppm) and a group of two signals in the spectral region  $\delta_H = 0 - 2$  ppm, which can be attributed to surface hydroxyl groups and weakly associated water [30–32]. In the case of sample AM-1 + 100 mg/g SA (Figure 5b), the signal of dimethylsilyl groups is dominant. CH<sub>2</sub> signals of SA and OH signals of water are observed as a broad signal in the region of 2.5 – 5 ppm. The signal of COOH groups of SA ( $\delta_H = 7$  ppm) is also broadened, probably due to exchange processes with protons molecules of strongly associated water. Signal with  $\delta_H = 12$  ppm due to the satellite of sample rotation at a magic angle with a frequency of about 10 kHz.

In the case of the A-300/AM-1 + 100 mg/g SA sample (Figure 5c), the spectra show signals of dimethylsilyl groups, CH<sub>2</sub> - and -COOH - acid groups, and strongly associated water. Its signal becomes dominant in composites activated with water (Figure 5d,e).

The processes of adsorption and desorption of biologically active substances immobilized on the surface of silica carriers are largely determined by the structure of the interfacial water. Due to the presence of four centers in the water molecule, through which it can form hydrogen bonds with other molecules (two polarized protons and two lone electron pairs of the oxygen atom), water belongs to strongly associated liquids. Many anomalous properties of liquid water can be explained

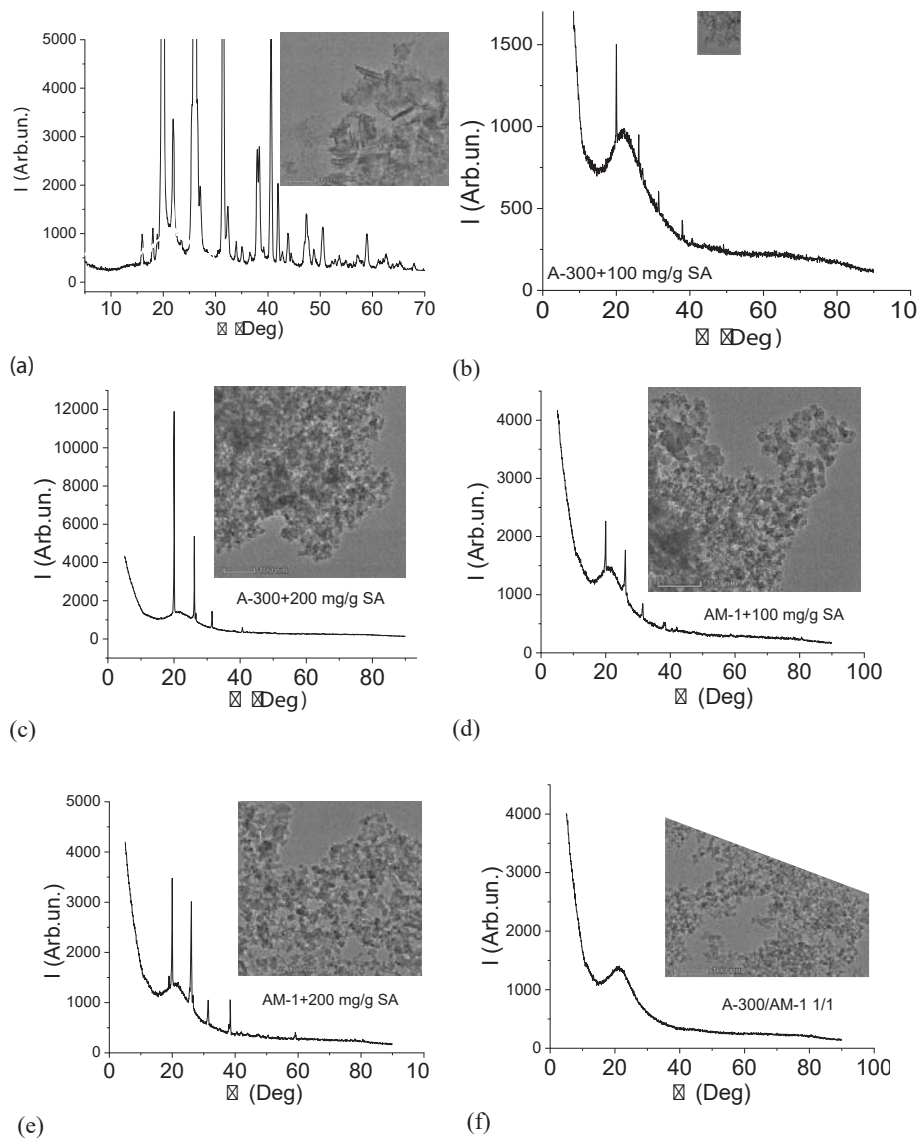


**Figure 2:** X-ray diffraction patterns of succinic acid (a), silica composites with SA (b-e) and AM-1 (f) (Diffractometer (Bruker AXS) in Bragg-Brentano geometry (Cu K $\alpha$ 1 radiation,  $\lambda = 0.15406$  nm). Diffraction data were typically collected at  $2\theta$  in the  $5-90^\circ$  range at a step of  $2^\circ/\text{min.}$ ) Combined with TEM micrographs of the corresponding samples (TECNAI G2 F30 microscope (FEI-Philips, operating voltage 300 kV).

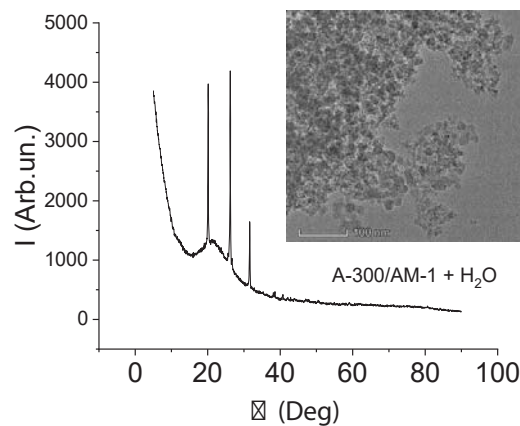


**Figure 3:** X-ray diffraction pattern and TEM micrograph of a composite prepared from a mixture of 1/1 A-300/AM-1 silicas with 100 mg/g of SA immobilized on the surface and subjected to additional mechanical treatment with 900 mg/g of H $_2$ O.

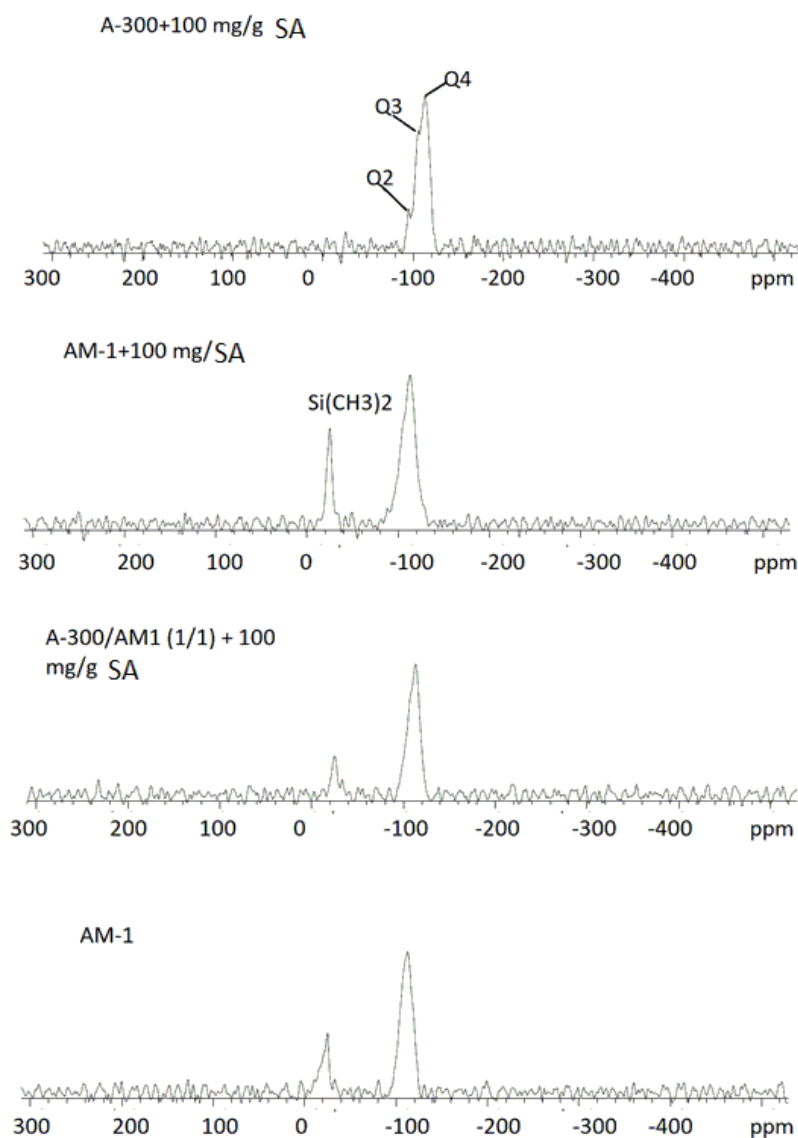


**Figure 4:**  $^{29}\text{Si}$  solid-state NMR spectra of A-300 and AM-1 silicas and their mixtures with SA immobilized on the surface, as well as the initial AM-1 (Agilent DD2 600 MHz NMR spectrometer (Agilent, USA, magnetic field strength 14.157 T))

by its cluster nature [33–37]. The cluster theory assumes that regions of high order in the network of hydrogen bonds in liquid water are separated by sufficiently extended regions of partially broken hydrogen bonds. As a result, the average number of hydrogen bonds per molecule in liquid water is 2.5–3 [38,39]. The NMR signal of such water has a chemical shift  $\delta_{\text{H}} = 5$  ppm, in contrast to completely ordered water in hexagonal ice ( $\delta_{\text{H}} = 7$  ppm). In a limited pore space or interparticle gaps of nonporous highly dispersed materials, the formation of extended ordered water structures is even more limited. Therefore, water can transform into a weakly associated form, which is characterized by a disordered arrangement of water molecules in the adsorption layer. In the NMR spectra, such water is observed as a signal in strong magnetic fields and has a chemical shift in the region  $\delta_{\text{H}} = 0\text{--}2$  ppm [32,39–41]. Such a strong dependence of the chemical shift of water protons on its association makes it possible to judge the structure of interfacial water using liquid NMR. In this case, the spectra

do not contain signals from the protons of the solid phase (adsorbents and frozen water).

Weakly associated water (WAW) has a number of properties characteristic of water in the supercritical state [41–43]. Its dielectric constant is almost an order of magnitude less than that of ordinary, strongly associated water (SAW), it mixes with both polar and non-polar substances, and its density is noticeably lower than that of liquid water. In the case of the formation of areas enriched with weakly associated water at the interfacial boundaries of medical composites, one can expect a noticeable effect on the interfacial transport of biologically active substances adsorbed on the mineral carrier.

Recorded at different temperatures  $^1\text{H}$  NMR spectra (Varian, Mercury 400 MHz) of water in moistened powders of hydrophilic (A-300) and hydrophobic (AM-1) silicas at a total water content in the samples (h) sufficient to fill a significant part of the interparticle space are shown in Figure 6. The measurements were carried out in air (Figure 6a,b) and with the

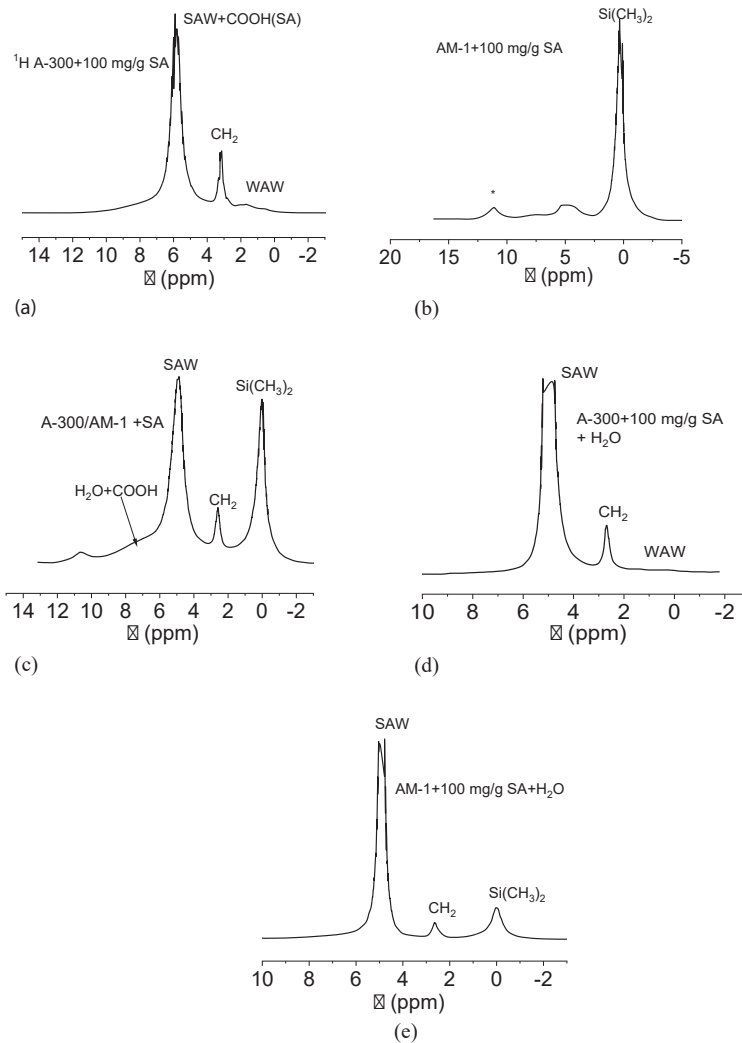


**Figure 5:**  $^1\text{H}$  solid-state NMR spectra of A-300 and AM-1 silicas and their mixtures with SA immobilized on the surface, as well as initial AM-1 (Agilent DD2 600 MHz NMR spectrometer (Agilent, USA, magnetic field strength 14.157 T)).

addition of a weakly polar organic solvent, deuteriochloroform (Figure 6c,d). The deuterated preparation was used to prevent the appearance of an additional proton signal in the spectra.

Recorded at different temperatures the type of spectra for hydrophilic A-300 (Figure 6a) and hydrophobic AM-1 (Figure 6b) silicas in air medium differ weakly. Water is recorded as a single signal with a chemical shift  $\delta_{\text{H}} > 4.5$  ppm, which corresponds to strongly associated water [37-39], each molecule of which participates in the formation of 2.5 - 3 hydrogen bonds. As the temperature decreases, the chemical shift of water increases due to an increase in the orderliness of the hydrogen bond network. In this case, the intensity of the water signal decreases due to the freezing of part of the adsorbed water.

Since the concentration of water in the samples is known, the values of the concentration of non-freezing water ( $C_{\text{uw}}$ ) at any temperature can be calculated from the intensities of the water signal (1):  $C_{\text{uw}} = I_{\text{T}}/I_{\text{T} > 273} \cdot h$  (mg/g). The process of freezing (fluctuation) of interfacial water localized in a solid porous matrix proceeds in accordance with changes in the Gibbs free energy as a result of the influence of the surface [44]. They are

the smaller, the farther from the surface is the studied layer of water. At  $T = 273$  K, water freezes, the properties of which do not differ from volumetric water, and when the temperature decreases (excluding the effect of overcooling), the layers of water close to the surface freeze, and besides for interfacial water the following proportion holds true:

$$\Delta G_{\text{ice}} = -0,036(273, 15 - T), \quad (1)$$

Where the numerical coefficient is a parameter related to the temperature coefficient of change in the Gibbs free energy for ice. Then, in accordance with the method described in detail in [37-39], it is possible to calculate the amount of strongly and weakly associated water (SBW and WBW, respectively), as well as the thermodynamic characteristics of these layers.

The interfacial energy ( $\gamma_s$ ) of solids or biopolymers was determined as the modulus of the total decrease of water-free energy, due to the presence of an internal water-polymer phase boundary according to the formula:

$$\gamma_S = -K \int_0^{C_{\text{uw}}^{\text{max}}} \Delta G(C_{\text{uw}}) dC_{\text{uw}}, \quad (2)$$

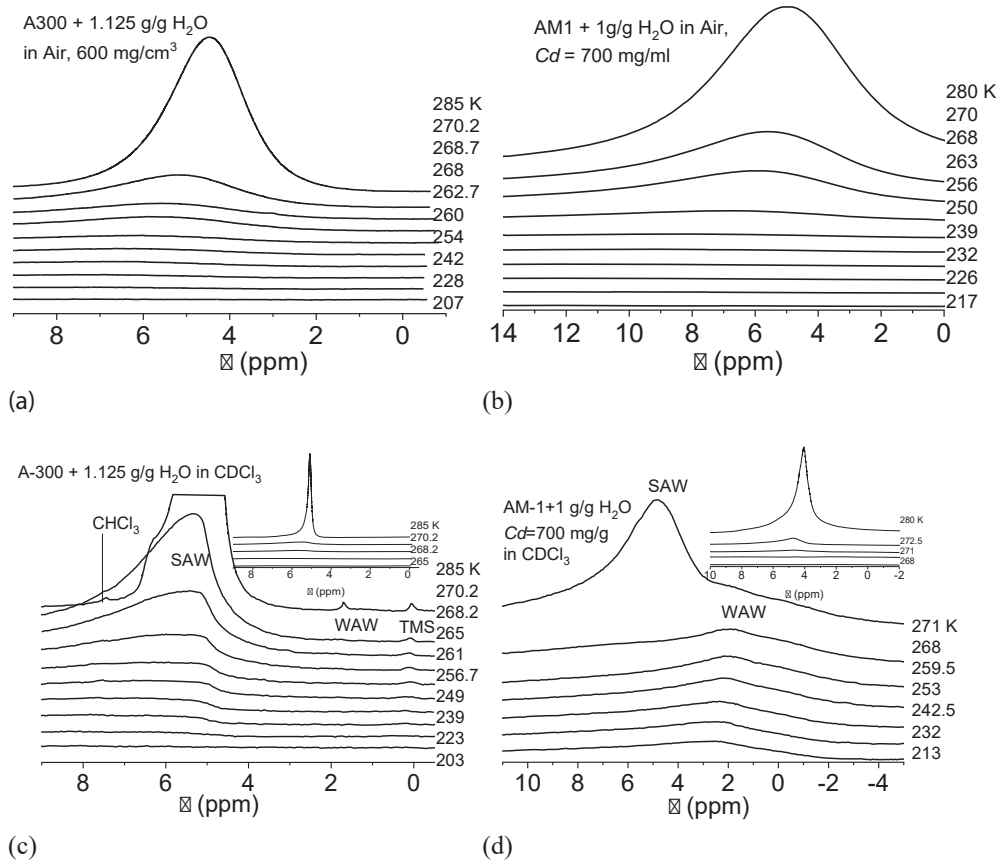


**Figure 6:** Recorded at different temperatures  $^1\text{H}$  NMR spectra of water adsorbed in the interparticle gaps of hydrophilic A-300 (a,c) and hydrophobic AM-1 (b,d) silicas in air (a,b) and in  $\text{CDCl}_3$  medium (c,d).

Where  $C_{\text{uw}}^{\text{max}} = h \cdot$

The Gibbs-Thomson equation can be used to determine the geometric dimensions limited by the solid surface of nanosized liquid aggregates [45,46], it relates the radius of spherical or cylindrical pores ( $R$ ) to the freezing point depression value:

$$\Delta T_m = T_m(R) - T_{m,\infty} = \frac{2\sigma_i T_{m,\infty}}{\Delta H_f \rho R} \quad (3)$$

Where  $T_m(R)$  is the melting temperature of ice localized in pores of radius  $R$ ,  $T_{m,\infty}$  is the melting temperature of bulk ice,  $\rho$  is the density of the solid phase,  $\sigma_{\text{sl}}$  is the interaction energy between solid object and liquid, and  $\Delta H_f$  is the volumetric enthalpy of melting.

The change in the Gibbs free energy ( $\Delta G$ ) and the value of the interfacial energy are calculated according to the formulas (1,2). The part of interfacial water for which the decrease in the Gibbs free energy  $\Delta G < 0.5$  kJ/mol was considered to be strongly bound. The dependencies of the concentration of non-freezing water on temperature ( $C_{\text{uw}}(T)$ ), the change in the Gibbs free energy on the concentration of non-freezing water, and the distribution of adsorbed water clusters over the radii are shown in Figure 7.

For A-300 (Figure 6c,d) in the  $\text{CDCl}_3$  medium (Figure 6c) strongly associated water (SAW) is observed as two signals with

chemical shifts  $\delta_{\text{H}} = 5$  and 6.5 ppm. At  $T = 285$  K, the spectra also show small signals of weakly associated water (WAW) ( $\delta_{\text{H}} = 2$  ppm), as well as signals of the deuterium-free chloroform component ( $\delta_{\text{H}} = 7.26$  ppm) and tetramethylsilane ( $\delta_{\text{H}} = 0$  ppm). For water adsorbed in the interparticle gaps of hydrophobic silica, the form of the spectra is more complicated (Figure 6d). Strongly associated water is observed only at  $T > 250$  K. In addition, at least two signals of weakly associated water with chemical shifts  $\delta_{\text{H}} = 0-2$  ppm are recorded. While the SAW signal decreases strongly with decreasing temperature, the intensity of the WAW signal changes only weakly. The concentration of weakly associated water in a wide temperature range is 10–20 mg/g (Figure 7a).

Characteristics of layers of non-freezing water – concentrations of strongly and weakly bound water ( $C_{\text{uw}}^{\text{S}}$  и  $C_{\text{uw}}^{\text{W}}$ , respectively), the maximum decrease in free energy in a layer of strongly bound water ( $\Delta G^{\text{S}}$ ), and the value of interfacial energy ( $\gamma_{\text{s}}$ ) for hydrated A-300 and AM-1 are given in Table 2. In this case, the interfacial energy determines the total decrease in free energy due to the presence of the phase boundary. It is determined by integrating the dependencies  $\Delta G(C_{\text{uw}})$  (Figure 6b) extrapolated to the coordinate axes. The concentrations of strongly (weakly) bound water are also determined from these dependencies, assuming that strongly bound (SBW) is that part of non-freezing water for which  $\Delta G < 0.5$  kJ/mol [37–39]. Therefore, it characterizes the sum of the entropy and enthalpy components of the adsorption interaction.



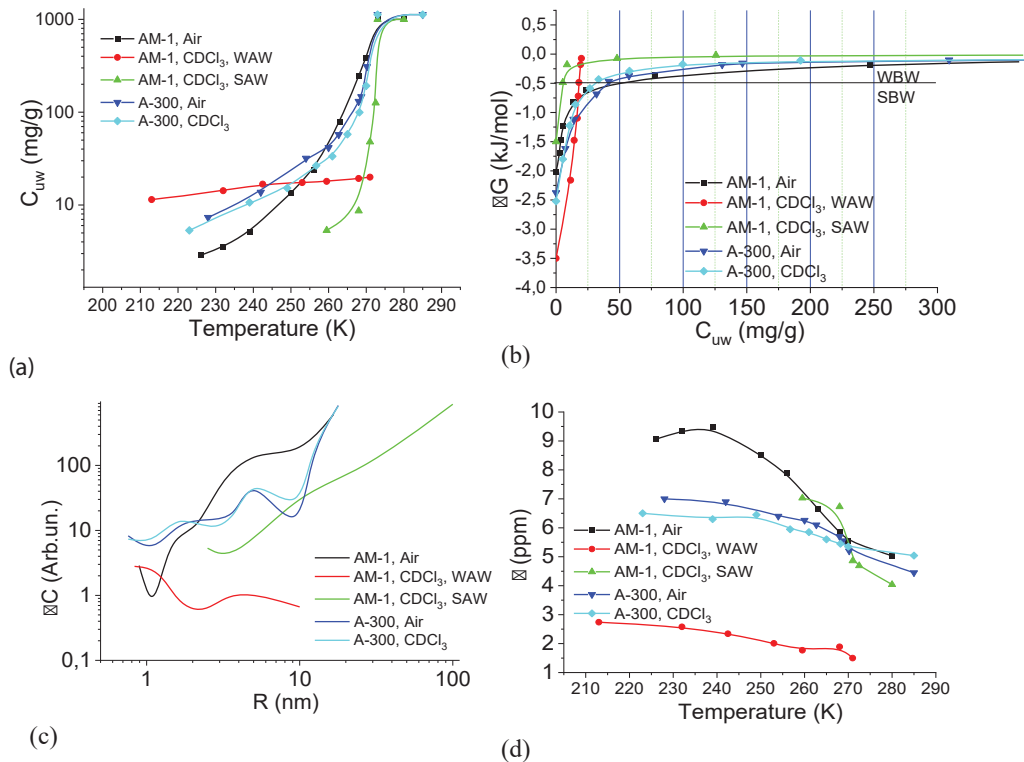


**Figure 7:** Temperature dependences of the concentration of non-freezing water (a), dependences of the change in the Gibbs free energy on the concentration of non-freezing water calculated on their basis (b), distribution of adsorbed water clusters over the radii (c), and temperature dependences of the chemical shift (d) for water adsorbed in interparticle gaps of hydrophilic and hydrophobic silicas.

**Table 2:** Characteristics of layers of non-freezing water in compacted samples A-300 and AM-1, in various media.

Sample	Medium	$C_{uw}^s$ (mg/g)	$C_{uw}^w$ (mg/g)	$\Delta G^s$ (kJ/mol)	$\gamma_s$ (J/g)
AM-1 0.7 g/cm <sup>3</sup> + 1.0 g/g H <sub>2</sub> O	Air	50	950	-2	8.2
	CDCl <sub>3</sub>	10	990	-1.5	1.3
A-300 0.6 g/cm <sup>3</sup> + 1.125 g/g H <sub>2</sub> O	Air	40	1085	-2.4	7.8
	CDCl <sub>3</sub>	30	1095	-2.5	6.5
AM-1/SA 0.6 g/cm <sup>3</sup> + 1.0 g/g H <sub>2</sub> O	Air	20	980	-2.2	4.8
	CDCl <sub>3</sub> WAW	18	5	-3.5	2.5
	CDCl <sub>3</sub> SAW	12	965	-3.5	3.2

**Note:**  $C_{uw}^s$  (mg/g) – the concentration of unfreezing strongly bound water;  $C_{uw}^w$  (mg/g) – the concentration of unfreezing weakly bound water;  $\Delta G^s$  (kJ/mol) – the change in Gibbs energy;  $\gamma_s$  (J/g) – the value of the interfacial energy.

According to Table 2, the value of  $\gamma_s$  for water in a hydrophobic environment ( $\gamma_s = 8.2$  J/g, hydrophobic hydration) is even greater than for a hydrophilic material ( $\gamma_s = 7.8$  J/g). It can be assumed that, compared with bulk water, the change in free energy in the interparticle gaps of silica is due to two main components – clustering, i.e. transformation of water into a system of clusters determined by the geometry of the interparticle gaps of water and the influence of the surface on the possibility of the formation of a spatial network of hydrogen bonds. Based on the results presented in Figure 7c, we can conclude that the radius of adsorbed water clusters in air for both types of materials is in the range  $R = 0.5 - 20$  nm. At the same time, for nanosilica A-300, the contribution from clusters with  $R = 2 - 20$  nm is greater (the  $\Delta C(R)$  curve is located higher), and for AM-1, from clusters with  $R = 0.5 - 2$  nm.

Replacing the air medium with the chloroform medium for the hydrophilic material leads to a slight decrease in the

interfacial energy from  $\gamma_s = 7.8$  to  $6.5$  J/g, which occurs due to the competition of chloroform with water when interacting with the silica surface. Only insignificant redistributions in the radii of adsorbed water clusters are observed on the curve  $\Delta C(R)$  (Figure 7c). In the case of hydrophobic silica in the  $CDCl_3$  medium, the value of  $\gamma_s$  decreases by more than six times, which indicates the active displacement of water from the interparticle gaps of the adsorbent and its replacement by chloroform. Accordingly, the average radius of clusters of strongly associated water adsorbed in interparticle gaps increases several times. Thus, in an entropy nonequilibrium system, such as hydrophobic silica, whose interparticle gaps are filled with water, its effective displacement is observed upon contact with a hydrophobic medium. In this case, about 10 mg/g of adsorbed water, localized mainly in voids of a small radius, passes into a weakly associated state characterized by a small chemical shift (Figures 6d,7d).

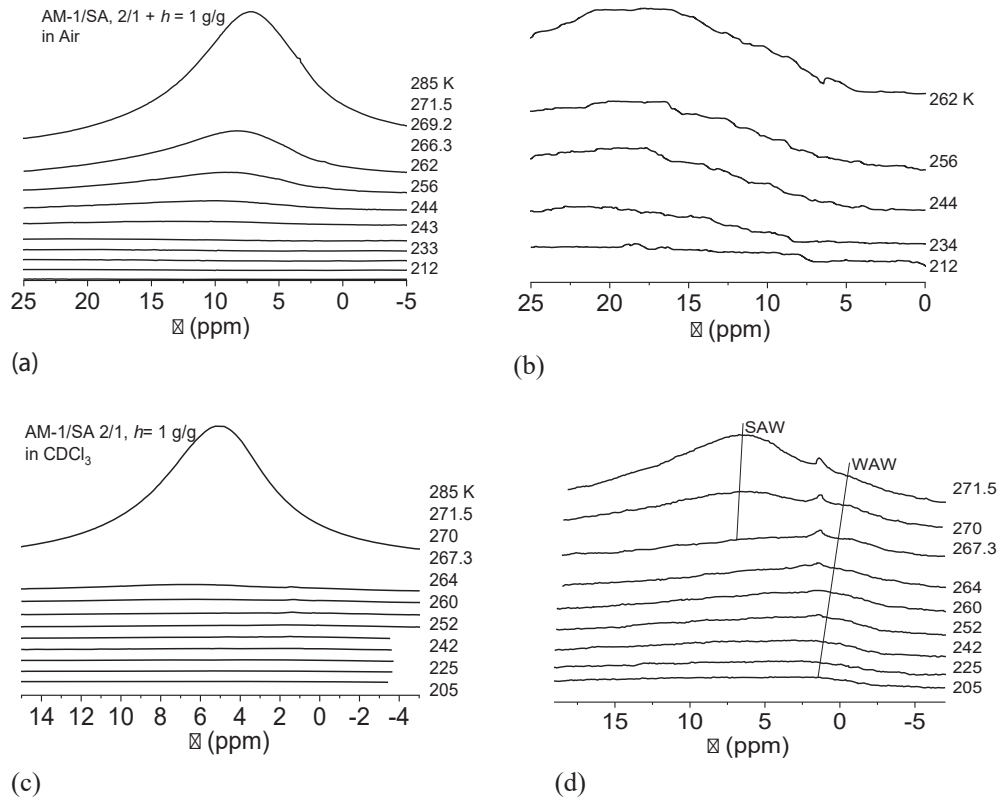


**Figure 8:** Recorded at different temperatures  $^1\text{H}$  NMR spectra of water adsorbed in the interparticle gaps of the AM-1/SA/ $\text{H}_2\text{O}$  (1/0.3/1.3) composite in air (a,b) and with the addition of deuteriochloroform (c,d).

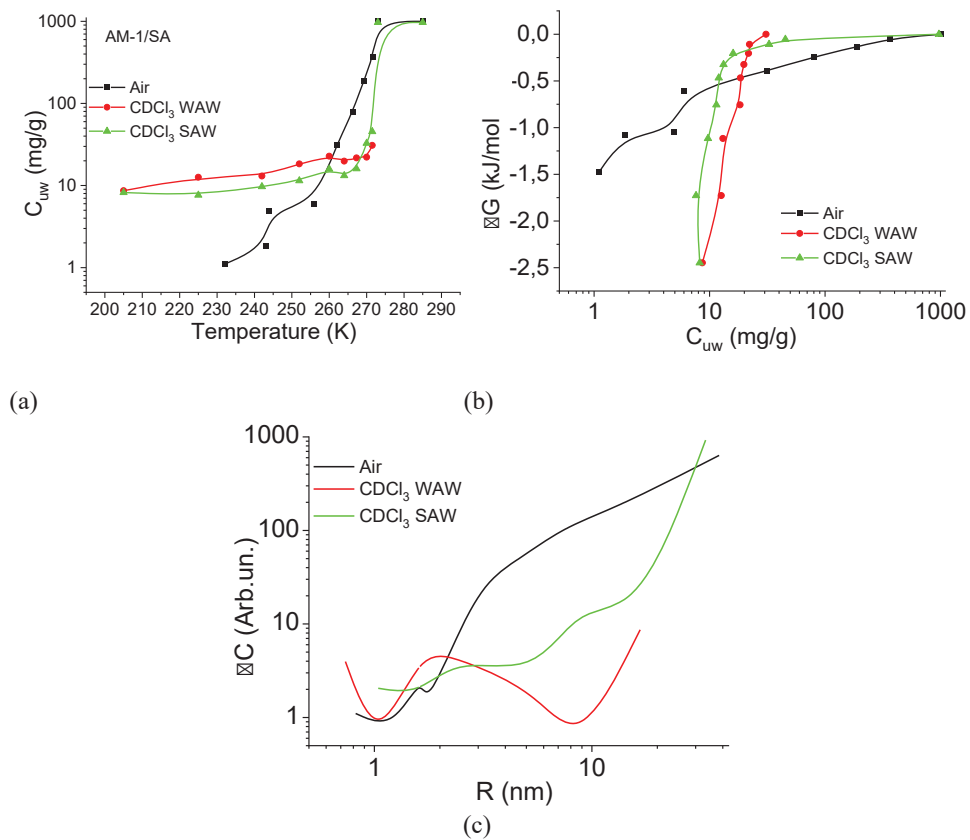


**Figure 9:** Temperature dependences of the concentration of non-freezing water (a), dependences of the change in the Gibbs free energy on the concentration of non-freezing water calculated on their basis (b), and the distribution of adsorbed water over the radii of clusters (c) for water adsorbed in the interparticle gaps of AM-1 with immobilized on surface of the SA.

For the studied systems, the temperature dependencies of the change in the chemical shift of adsorbed water are shown in Figure 7d. The main changes in the chemical shift are observed at temperatures  $T = 255 - 285$  K when the bulk of the adsorbed water melts. For hydrophilic silica in air at low temperatures, anomalously high values are recorded  $\delta_H$ . Perhaps they are associated with the formation of hydrogen-bonded water complexes at the silica-ice interface with the participation of dissociated protons of silanol groups. For other systems, the range of chemical shifts is from 4.5 to 7 ppm, which is typical for a partially broken network of hydrogen bonds of adsorbed water in a quasi-liquid state [38].

For the AM-1/SA/H<sub>2</sub>O composite system in the air (Figure 8a,b), the chemical shift of adsorbed water shifts to large values. At  $T = 280$  K, the chemical shift of water is  $\delta_H = 7$  ppm, and as the temperature decreases, it increases almost to  $\delta_H = 20$  ppm (Figure 8b). This is probably due to the predominant adsorption of water on the surface of AM-1, which has inclusions of SA clusters. Owing to the presence of carboxyl groups in SA molecules, they can act as binding centers with clusters of water adsorbed on the surface. Such a large chemical shift in frozen systems indicates the possibility of forming very strong (close to symmetrical) hydrogen bonds with acid molecules. It should be noted that the absence of SA methylene groups in the spectra can be interpreted as its existence exclusively in the solid state and its low solubility in clustered water.

In the presence of CDCl<sub>3</sub>, the type of the spectra of the AM-1/SA/H<sub>2</sub>O composite system changes (Figure 8c,d). The value of the chemical shift of adsorbed water decreases, most of it freezes at relatively higher temperatures, and at low temperatures, at least two signals of weakly associated water with  $\delta_H = 1 - 2$  ppm are recorded in the spectra. At  $T < 267$  K, the WAW signal becomes dominant as virtually all of the SAW freezes.

Temperature dependencies of the concentration of non-freezing water ( $C_{uw}(T)$ ), built on the basis of the change in the intensity of the water signal during heating of the sample, pre-cooled to  $T = 200 - 210$  K (a), the change in the Gibbs free energy ( $\Delta G$ ) on the concentration of non-freezing water (b) and distributions over the radii of adsorbed water clusters calculated in accordance with formula (3) (c) are shown in Figure 9. According to the data in the table, the interfacial energy is controlled predominantly by the concentration of strongly bound water. For the AM-1/SA/H<sub>2</sub>O composite system in air, the interfacial energy is  $\gamma_s = 4.8$  J/g, which is 2.5 times less than for a completely hydrophobic material. Accordingly, water is predominantly a part of clusters with a relatively larger radius (Figure 9c). Replacing the air environment with a chloroform environment leads to a significant decrease in the value of the interfacial energy of strongly associated water. This is true for both types of the studied systems (AM-1/H<sub>2</sub>O and AM-1/SA/H<sub>2</sub>O). However, at low temperatures, the contribution to the interfacial energy from weakly associated water increases, the amount of which does not exceed 2% of the total amount of nonfreezing water (Figure 9a).

## Conclusion

Combined mechanical grinding of crystalline succinic acid with hydrophobic or hydrophilic silica (or their mixture) results

in the formation of composite systems in which SA is uniformly distributed in the interparticle gaps of silicas and occurs in the form of nanoscale predominantly amorphous clusters. For silicas and their mixtures, X-ray diffraction patterns also show the signal of SA crystallites. Additional mechanical treatment of the composites with water practically does not change the ratio of the amorphous and crystalline components of the SA in the surface layer, which indicates the poor solubility of the SA immobilized on the silica surface in clustered water. This is also confirmed by the liquid NMR data, according to which there is no signal from the methylene groups of SA in the spectra.

All composites, regardless of the content of SA, treatment with water, and the ratio of the hydrophobic and hydrophilic components, retain a high adsorption capacity with respect to nitrogen. The BET-specific surface of the composites remains at the level of 150 - 200 m<sup>2</sup>/g.

Hydrated forms of hydrophobic silica AM-1 retain the ability to interact with non-polar substances. Using chloroform as an example, it was shown that even at  $h = 1$  g/g, chloroform displaces part of the water from the interparticle space, which manifests itself in a decrease in the interfacial energy of water due to the formation of surface water clusters with a large radius.

The hydrophobic silica surface stabilizes the weakly associated form of water, the amount of which can reach 20 mg/g. Despite the relatively low content of WAW, it can have a very significant effect on interfacial transport, because it is focused at the interface between the aqueous and solid mineral phases.

## References

- Ashton S, Song YH, Nolan J, Cadogan E, Murray J, Odedra R, Foster J, Hall PA, Low S, Taylor P, Ellston R, Polanska UM, Wilson J, Howes C, Smith A, Goodwin RJ, Swales JG, Strittmatter N, Takáts Z, Nilsson A, Andren P, Trueman D, Walker M, Reimer CL, Troiano G, Parsons D, De Witt D, Ashford M, Hrkach J, Zale S, Jewsbury PJ, Barry ST. Aurora kinase inhibitor nanoparticles target tumors with favorable therapeutic index in vivo. *Sci Transl Med*. 2016 Feb 10; 8(325):325ra17. doi: 10.1126/scitranslmed.aad2355. PMID: 26865565.
- Bawa R, Audette GF, Reese BE, editors. *Handbook of clinical nanomedicine: law, business, regulation, safety, and risk*. New York: Jenny Stanford Publishing. 2016; 1502.
- Nair M, Guduru R, Liang P, Hong J, Sagar V, Khizroev S. Externally controlled on-demand release of anti-HIV drug using magneto-electric nanoparticles as carriers. *Nat Commun*. 2013; 4:1707. doi: 10.1038/ncomms2717. Erratum in: *Nat Commun*. 2013; 4:2729. PMID: 23591874.
- Ward EM, Sherman RL, Henley SJ, Jemal A, Siegel DA, Feuer EJ, Firth AU, Kohler BA, Scott S, Ma J, Anderson RN, Benard V, Cronin KA. Annual Report to the Nation on the Status of Cancer, Featuring Cancer in Men and Women Age 20-49 Years. *J Natl Cancer Inst*. 2019 Dec 1; 111(12):1279-1297. doi: 10.1093/jnci/djz106. PMID: 31145458; PMCID: PMC6910179.
- Yang J, Wang Z, Zong S, Chen H, Zhang R, Cui Y. Dual-mode tracking of tumor-cell-specific drug delivery using fluorescence and label-free SERS techniques. *Biosens Bioelectron*. 2014 Jan 15; 51:82-9. doi: 10.1016/j.bios.2013.07.034. Epub 2013 Jul 26. PMID: 23939474.
- Gray MD, Lyon PC, Mannaris C, Folkes LK, Stratford M, Campo L, Chung DYF, Scott S, Anderson M, Goldin R, Carlisle R, Wu F, Middleton MR, Gleeson FV, Coussios CC. Focused Ultrasound Hyperthermia for Targeted Drug Release from Thermosensitive Liposomes: Results from a Phase I Trial. *Radiology*. 2019 Apr; 291(1):232-238. doi: 10.1148/radiol.2018181445. Epub 2019 Jan 15. PMID: 30644817.



7. Turov VV, Krupskaya TV, Guzenko NV, Borysenko MV, Nychiporuk YuM, Gun'ko VM. Controlled confined space effects on clustered water bound to hydrophobic nanosilica with nonpolar and polar co-adsorbates. *Colloids Surfaces A Physicochem Eng Aspects*. 2022; 644:128919. doi:10.1016/j.colsurfa.2022.128919.
8. Turov VV, Gerashchenko II, Krupskaya TV, Suvorova LA. Nanochemistry in solving problems of exo- and endoecology. *Stavropol: Zebra*. 2017; 315.
9. Gun'ko VM, Turov VV, Pakhlov EM, Krupskaya TV, Borysenko MV, Kartel MT, Charnas B. Water Interactions with Hydrophobic versus Hydrophilic Nanosilica. *Langmuir*. 2018 Oct 9; 34(40):12145-12153. doi: 10.1021/acs.langmuir.8b03110. Epub 2018 Sep 25. PMID: 30212631.
10. Gun'ko VM, Turov VV, Pakhlov EM, Matkovskiy AK, Krupskaya TV, Kartel MT, Charnas B. Blends of amorphous/crystalline nanoalumina and hydrophobic amorphous nanosilica. *J Non-Cryst Solids*. 2018; 500:351-358. doi:10.1016/j.jnoncrysol.2018.08.020.
11. Muller VM. Theory of reversible coagulation. *Colloid J*. 1996; T. 58:5; 634-647.
12. Efremov IF. Periodic colloid structures. *L. Chemistry*. 1971; 192.
13. Smay JE, Gratson GM, Shepherd RF, Cesarano J III, Lewis JA. Directed colloidal assembly of 3D periodic structures. *Adv Mater*. 2002; 14(18):1279-1283. doi:10.1002/1521-4095(20020916)14:18<1279::AID-ADMA1279>3.0.CO;2-A.
14. Sun S, Xia Q, Feng D, Ru H. Adsorption effects of polyethylene imine on the rheological properties for robocasting. *J. Mat. Sci*. 2022; 57(4):3057-3066. doi:10.1007/s10853-021-06802-4
15. Turov VV, Krupskaya TV. Influence of mechanical loads on the state of water in the hydrophobic environment of methyl silica particles // *Theor. Exp. Chem*. 2022; 58:1; 48-53. doi:10.1007/s11237-022-09721-w
16. Turov VV, Gun'ko VM, Turova AA, Morozova LP, Voronin EF. Interfacial behavior of concentrated HCl solution and water clustered at a surface of nanosilica in weakly polar solvents media // *Colloids Surf. A: Physicochem. Engin. Aspects*. 2011; 390(1-3):48-55. doi.org/10.1016/j.colsurfa.2011.08.053
17. Gun'ko VM, Turov VV, Turov AV. Hydrogen peroxide – water mixture bound to nanostructured silica. *Chem. Phys. Lett*. 2012; 531:132-137. doi:10.1016/j.cplett.2012.01.090
18. Fumagalli C. Succinic acid and succinic anhydride. In *Kirk-Othmer Encyclopedia of Chemical Technology*, 4th ed. Kroschwitz JI, Howe-Grant M, Eds. Wiley: New York. NY. USA. 1997; 22:1074-1102.
19. Bertuzzi A, Gandolfi A, Salinari S, Mingrone G, Greco A.V. Pharmacokinetics of dicarboxylic acids in man. *Eng Med Biol*. 1994; 13(4):472-478. doi:10.1109/51.310987
20. Zeikus JG, Jain MK, Elankovan P. Biotechnology of succinic acid production and markets for derived industrial products. *Appl. Microbiol. Biotechnol*. 1999; 51(5):545-552. doi:10.1007/s002530051431
21. Sheng Z, Tingting B, Xuanying C, Xiangxiang W, Mengdi L. Separation of succinic acid from aqueous solution by macroporous resin adsorption. *J. Chem. Eng*. 2016; 61(2):856-864. doi:10.1021/acs.jced.5b00713
22. Chen SW, Xin Q, Kong WX, Min L, Li JF. Anxiolytic-like effect of succinic acid in mice. *Life Sci*. 2003 Nov 7; 73(25):3257-64. doi: 10.1016/j.lfs.2003.06.017. PMID: 14561530.
23. Narayan S, Devi RS, Jainu M, Sabitha KE, Shyamala Devi CS. Protective effect of a polyherbal drug, ambren in ethanol induced gastric mucosal lesions in experimental rats. *Indian J. Pharmacol*. 2004; 36(1): 34-37.
24. Mironyuk IF, Gun'ko VM, Vasylyeva HV, Goncharuk OV, Tatarchuk T, Mandzyuk VI, Bezruka NA, Dmytrotsa TV. Effects of enhanced clusterization of water at a surface of partially silylated nanosilica on adsorption of cations and anions from aqueous media. *Microporous and Mesoporous Materials*. 2019; 277:95-104. doi:10.1016/j.micromeso.2018.10.016
25. Bergna HE, Roberts WO. *Colloidal Silica: Fundamentals and Applications*, CRC Press, Boca Raton. 2006; 944.
26. Aerosil - Fumed Silica, Technical Overview, Evonik Ind. Hanau. 2015.
27. Gun'ko VM, Turov VV, Pakhlov EM, Krupskaya TV, Charnas B. Effect of water content on the characteristics of hydro-compacted nanosilica. *Appl. Surf. Sci*. 2018; 459:171-178. <https://doi.org/10.1016/j.apsusc.2018.07.213>
28. Krupskaya TV, Turov VV, Barvinchenko VM, Filatova KO, Suvorova LA, Iraci G, Kartel MT. Influence of the "wetting-drying" compaction on the adsorptive characteristics of nanosilica A-300. *Ads. Sci. & Technol*. 2017; 36(1-2). doi:10.1177/0263617417691768
29. Krupskaya TV, Turov VV, Barvinchenko VM, Filatova KO, Suvorova LA, Kartel MT. Pat. On useful model N 105151 Ukraine. The method of compacting nanosilica. *Publ. 10.03.2016. Bul. N 3. Utility Model Patent N 105151*.
30. Chung IS, Maciel GE. Probing Hydrogen Bonding at the Local Environment of Silanols on Silica Surfaces via Nuclear Spin Cross Polarization Dynamics. *J. Am Chem Soc*. 1996; 118(2):401-406. doi:10.1021/ja951550d
31. Chang IS, Kinney DR, Maciel GE. Interior Hydroxyl of the Silica Gel System as Studied by <sup>29</sup>Si CP-MAS NMR Spectroscopy. *J. Am Chem. Soc*. 1993; 115(19):8695-8705. doi:10.1021/ja00072a024
32. Gun'ko VM, Turov VV. Nuclear Magnetic Resonance Studies of Interfacial Phenomena. *New York: Taylor & Francis*. 2013; 1040. doi:10.1201/b14202
33. Ratcliffe CI, Irish DE. Vibrational spectral studies of solutions at elevated temperatures and pressures. 5. Raman studies of liquid water up to 300°C. *J. Phys. Chem*. 1982; 86:25; 4897-4905. doi:10.1021/j100222a013
34. Chaplin MF. A proposal for the structuring of water. *Biophys Chem*. 2000 Jan 24; 83(3):211-21. doi: 10.1016/s0301-4622(99)00142-8. PMID: 10647851.
35. Su JT, Xu X, Goddard III W.A. Accurate Energies and Structures for Large Water Clusters Using the X3LYP Hybrid Density Functional. *J. Phys. Chem. A*: 2004; 108(47):10518-10526. doi:10.1021/jp047502+
36. James T, Wales DJ, Hernandez-Rojas J. Global minima for water clusters (H<sub>2</sub>O)<sub>n</sub>, n ≤ 21, described by a five-site empirical potential. *Chem. Phys. Lett*. 2005; 415(4-6):302-307. doi:10.1016/j.cplett.2005.09.019
37. Xantheas SS, Burnham CJ, Harrison RJ. Development of Transferable Interaction Models for Water. II. Accurate Energetics of the First Few Water Clusters from First Principles. *J. Chem. Phys*. 2002; 116:4; 1493-1499. doi:10.1063/1.1423941
38. Turov VV, Gunko VM. Clustered water and ways of its use. *Kyiv, Naukova Dumka*. 2011; 316.
39. Gunko VM, Turov VV, Gorbik PP. Water at the interface. *Kyiv, Naukova Dumka*. 2009; 694.
40. Gun'ko VM, Turov VV, Bogatyrev VM, Zarko VI, Leboda R, Goncharuk EV, Novza AA, Turov AV, Chuiko AA. Unusual properties of water at hydrophilic/hydrophobic interfaces. *Adv Colloid Interface Sci*. 2005 Dec 30; 118(1-3):125-72. doi: 10.1016/j.cis.2005.07.003. Epub 2005 Oct 6. PMID: 16213452.
41. Wagner W., Pruss A. The IAPWS Formulation 1995 for the Thermodynamic Properties of Ordinary Water Substance for General and Scientific Use. *J. Phys. Chem. Ref. Data*. 2002; 31(2):387-535. doi:10.1063/1.1461829
42. Galkin AA, Lunin VV. Water in sub- and supercritical states as a universal medium for the implementation of chemical reactions. *Uspekhi Khimii*. 2005; 74: 1. 1; 24-40.
43. Marsall W. Jones E. Liquid-vapor critical temperatures of aqueous electrolyte solutions. *J. Inorg. Nucl. Chem*. 1974; 36(10):2313-2318. doi:10.1016/0022-1902(74)80275-7
44. Glushko VP. *Thermodynamic Properties of Individual Substances*. Moscow: Nauka. 1978; 495.
45. Aksnes DW, Forl K, Kimtys L. Pore size distribution in mesoporous materials as studied by <sup>1</sup>H NMR. *Phys. Chem. Chem. Phys*. 2001; 3(15):3203-3207. doi:10.1039/b103228n
46. Petrov OV, Furó I. NMR cryoporometry: Principles, applications and potential. *Progr. NMR Spectroscopy*. 2009; 54(2):97-122. doi:10.1016/j.pnmrs.2008.06.001